Ionotropic glutamate receptor (iGluR)-like channels mediate MAMP-induced calcium influx in Arabidopsis thaliana

Mark Kwaaitaal, Rik Huisman, Jens Maintz, Anja Reinstädler, Ralph Panstruga

IONOTROPIC GLUTAMATE RECEPTOR (iGluR)-LIKE CHANNELS MEDIATE MAMP-INDUCED CALCIUM INFLUX IN *ARABIDOPSIS THALIANA*

Mark Kwaaitaal[*], Rik Huisman[*], Jens Maintz[*], Anja Reinstädler[*] and Ralph Panstruga[*,§]

[*] Max-Planck Institute for Plant Breeding Research, Department of Plant-Microbe Interactions, Carl-von-Linné-Weg 10, 50829 Köln, Germany
[§] RWTH Aachen University, Institute for Biology 1, Unit of Plant Molecular Cell Biology, 52056 Aachen. Germany

Address correspondence to Ralph Panstruga, RWTH Aachen University, Institute for Biology 1, Unit of Plant Molecular Cell Biology, Worringer Weg 1, 52056 Aachen. Germany, Tel. +49 (0) 241 8026655, Fax.+49 (0) 241 8022637, Email: panstruga@bio1.rwth-aachen.de

Running head: iGluR-like channels mediate MAMP-triggered calcium influx in *Arabidopsis*

Key words

Calcium channel, calcium signature, elicitor, ionotropic glutamate receptor channel, microbe-associated molecular pattern, plant immunity

Abbreviations

CICR	calcium-induced calcium release
CNGC	cyclic nucleotide-gated channel
HR	hypersensitive response
iGluR	ionotropic glutamate receptor
MAPK	mitogen-activated protein kinase
ROS	reactive oxygen species
RR	Ruthenium Red
VGCC	voltage-gated calcium channel

Synopsis

Binding of specific microbial epitopes (microbe-associated molecular patterns, MAMPs) to pattern recognition receptors (PRRs) and subsequent receptor kinase activation are key steps in plant innate immunity. One of the earliest detectable events after MAMP perception is a rapid and transient rise in cytosolic calcium (Ca^{2+}) levels. In plants, knowledge about the signaling events leading to Ca^{2+} influx and on the molecular identity of the channels involved is scarce. We used a transgenic *Arabidopsis thaliana* line stably expressing the luminescent aequorin Ca^{2+} biosensor to monitor pharmacological interference with Ca^{2+} signatures following treatment with the bacterial peptide MAMPs flg22 and elf18 and the fungal carbohydrate MAMP chitin. Using a comprehensive set of compounds known to impede Ca^{2+} transport processes in plants and animals we found strong evidence for a prominent role of amino acid-controlled Ca^{2+} fluxes, probably through ionotropic glutamate receptor (iGluR)-like channels. Interference with amino acid-mediated Ca^{2+} fluxes modulates MAMP-triggered mitogen-activated protein kinase (MAPK) activity and affects MAMP-induced accumulation of defense gene transcripts. We conclude that the initiation of innate immune responses upon flg22, elf18 and chitin recognition involves apoplastic Ca^{2+} influx via iGluR-like channels.

Introduction

Eukaryotic organisms possess an extensive array of receptor proteins to sense their environment, including the presence of benign or hostile (micro-) organisms. Major pathways for the relay of exogenous signals to the cytoplasm/nucleus invoke pattern recognition receptors (PRRs) that sense specific microbial epitopes termed microbe-associated molecular patterns (MAMPs). PRRs play a key role in plant innate immunity by the activation of defense response pathways upon MAMP sensing (MAMP-triggered immunity) [1] Examples of PRRs comprise FLAGELLIN SENSING2 (FLS2), ELONGATION FACTOR-Thermo unstable (EF-Tu) RECEPTOR (EFR) and CHITIN ELICITOR RECEPTOR KINASE1 (CERK1). FLS2 and EFR activate downstream signaling after detection of 22 and 18 amino acid-long epitopes of bacterial flagellin (flg22) and EF-Tu (elf18), respectively [2, 3]. CERK1 is essential for the recognition of chitin polymers, major constituents of the fungal cell wall [4]. Detection of MAMPs by PRRs typically results in a series of early cellular responses such as fluxes of calcium (Ca^{2+}) and other ions, the generation of reactive oxygen species (ROS), the initiation of mitogen-activated protein kinase cascades (MAPK(K/KK)) and the activation of Ca^{2+}-dependent protein kinases (CDPKs) [1]. Despite their canonical occurrence, the functional role of these archetypal responses in plant innate immunity remains largely obscure.

Ca^{2+} acts as a second messenger in response to many biotic and abiotic stimuli, e.g. microbial attack, symbiosis, heat shock, cold shock, osmotic stress, oxidative stress, light conditions and abscisic acid [1, 5, 6]. These different cues each induce their own specific Ca^{2+} signatures; transients that differ in timing as well as the number and magnitude of Ca^{2+} spikes. The transient increase of cytosolic [Ca^{2+}] results from passive Ca^{2+} influx from the apoplast or intracellular Ca^{2+} stores through dedicated channels [7]. Since Ca^{2+} is cytotoxic, low concentrations are maintained in the cytosol and nucleus of resting cells. H^+/Ca^{2+}-exchangers and ATP-dependent Ca^{2+} pumps (Ca^{2+}-ATPases) expel Ca^{2+} in an energy-dependent process from the cytosol to the extracellular space and into intracellular compartments such as the vacuole and the endoplasmic reticulum (ER). As a result, the [Ca^{2+}] in the apoplast and intracellular stores is up to 20,000 times higher than in the cytosol. The combination of this concentration gradient and a proton-based electrochemical gradient over cellular membranes [8] is the driving force for the stimulus-dependent influx of Ca^{2+} into the cytosol [7].

Genome-wide comparisons revealed large differences between families for channel candidates mediating Ca^{2+} import in plants and mammals [8-10]. Genes encoding obvious orthologs of some major classes of mammalian channels are lacking in plants (ryanodine receptor channels, $InsP_3$-activated receptor channels and voltage-gated channels), while the family of cyclic nucleotide-gated channels (CNGCs) is expanded in plants. Even though sequence-related genes are missing, electrophysiological experiments indicated the presence of voltage-gated Ca^{2+} channels in plant organelles and cells [11, 12]. Apparently, a unique and sequence-diverged set of proteins contributes to the control of Ca^{2+} influx into plant cells.

CNGCs comprise a family of twenty ligand-gated ion channels in *Arabidopsis thaliana* [8]. CNGCs are gated by cyclic nucleotides (cNTPs) [13, 14]. Several CNGCs have been functionally linked to plant immunity. For example, the *defense no death* (*dnd*) class of mutants has a reduced ability to initiate a hypersensitive response (HR) to avirulent bacteria. *DND1* and *DND2* encode two CGNC paralogs (CNGC2 and CNGC4) [15, 16]. In addition to the altered cell death phenotype, *cngc2* knockout plants show an altered Ca^{2+} signature in response to the bacterial MAMP lipopolysaccharide (LPS) [13].

The second major class of putative ligand-gated Ca^{2+}-permeable channels in plants comprises the ionotropic glutamate receptor-like channels (iGluRs). They function as heterotetramers and are best known for their role in neurotransmission in vertebrates [17]. iGluR-like channels possess a large N-terminal extracellular domain, three transmembrane regions, a hydrophobic loop defining the pore region and a cytosolic C-terminal domain. Especially the pore region of iGluR-like channels differs strongly between plants and animals [18, 19]. However, ion pore transplantation experiments have shown that the pores of two *Arabidopsis* iGluRs (AtiGluR1.1 and AtiGluR1.4) are permeable to Ca^{2+}, Na^+ and K^+ [18]. Twenty iGluRs are encoded in the *Arabidopsis* genome [9, 10, 19]. They are involved in various processes ranging from biotic and abiotic stress responses [20] to pollen tube

growth [21] and hypocotyl elongation [22]. Recently, Ca^{2+} influx and NO production triggered by the proteinaceous oomycete MAMP cryptogein were also found to involve iGluR-like channels [23].

Here we used a transgenic *Arabidopsis thaliana* line expressing the aequorin Ca^{2+} biosensor to investigate intracellular Ca^{2+} signatures in response to three different, well-characterized MAMPs (flg22, elf18 and chitin). We conducted pharmacological interference with the MAMP-triggered Ca^{2+} influx using a comprehensive set of compounds known to impede various classes of Ca^{2+} channels. Besides the actual Ca^{2+} signatures, we used MAMP-induced downstream responses such as MAPK activation and accumulation of defense gene transcripts as additional readouts for Ca^{2+} channel modulation. Our findings support a crucial role of iGluR-like channels in the generation of MAMP-triggered Ca^{2+} signatures and provide evidence for a critical role for MAMP-induced Ca^{2+} signaling in defense gene activation.

Experimental

Plant growth

Arabidopsis Col-0 seeds or Col-0 35S::aequorin seeds [24] were surface-sterilized once with 70% ethanol and subsequently twice with 100% ethanol before drying. Dry seeds were transferred to a 96-well plate (Perkin-Elmer, Waltham, USA; 1-2 seeds per well) containing 100 µl 1x MS including vitamins (DUCHEFA, Haarlem, the Netherlands) with 0,25% sucrose. The seedlings were grown for 11-12 days with 16 hours light (21 ^{0}C), 8 hours dark (19 ^{0}C) before further study.

Chemicals

Unless stated otherwise, chemicals were obtained from SIGMA (Munich, Germany) or Tocris Biosciences (Ellisville, USA). Stock solutions were prepared in ddH_2O except for CNQX, U73122 and nifedipine, which were dissolved in DMSO. The influence of the solvent DMSO in the final concentration after chemical dilution was tested as an additional control.

Ca^{2+} measurements using the aequorin biosensor

After 11-12 days the growth medium was removed from the aequorin expressing seedlings and replaced by 100 µl ddH_20 containing 10 µM coelenterazine (BIOSYNTH, Staad, Switzerland), diluted from a 5 mM stock solution in methanol, and incubated overnight in the dark. The next day, the medium was replaced by 100 µl ddH_20 and the seedlings were incubated for 30 min in the dark. For the compound treatments, 10-times concentrated stocks in water were prepared and added to the coelenterazine-loaded seedlings. The seedlings were preincubated for one hour before starting the measurements. Elf18 and flg22 were present as 10 or 1 mM stock solutions in water stored at -80 ^{0}C and used freshly. Chitin solution was prepared by intermittently grinding (for 15-20 minutes) 10 mg crab or shrimp shell (SIGMA, Munich, Germany) powder in 1 ml ddH_20 with a pestle and subsequent vortexing and heating the solution to 60 ^{0}C. Undissolved particles were removed by centrifugation (15 minutes, 13000 rpm) and the clear supernatant was used for the experiments. The measurements were performed in a 96-well Centro LB960 luminometer system (Berthold Technologies, Bad Wildbad, Germany). Half a plate was measured in one go. Luminescence from one single well was detected for 0,25 seconds and each well was measured every 30 seconds. After 2 minutes (4 measurements), 5-times concentrated MAMP was automatically added to a final concentration of 1 µM flg22, 1 µM elf18 or 0,1 mg/ml chitin. After addition, the luminescence was followed for an additional 40 minutes. The second half of the plate was run in the same manner. Finally, for calculation of Ca^{2+} concentrations, 100 µl 2 M $CaCl_2$ in 20% ethanol was added to each well using the injectors of the system and the luminescence was measured for 0,25s per well with one measurement per well every 63 seconds. The luminescence was followed for 30 minutes. Ca^{2+} concentrations were calculated according to Rentel and Knight (2004)[25].

Per treatment 4 to 6 individual wells were averaged. Ca^{2+} transients were compared between treatments within one experiment unless stated otherwise and at least three biological replicates per compound were performed. Unless stated otherwise, the data were normalized to background Ca^{2+} levels and represented as a $\Delta[Ca^{2+}]$ value to compensate for background variations between measurements. Owing to the low molecular mass of aequorin (22 kDa) and its presumed passive

transfer into the nucleus, we expect the *Arabidopsis* reporter line to monitor the combined cytoplasmic and nuclear (here referred to as intracellular) Ca^{2+} pool. Statistical significance of differences was evaluated by comparing average calcium responses of biological replicates of treated samples with non-treated control samples using a two-sided Student's t-test with unequal variances.

MAPK assays

The MAPK assays were performed essentially as previously described [26].

Quantitative RT-PCR

Preparation, pretreatment and MAMP addition to the seedlings was identical as described for the MAPK assays. Time point 0 was harvested before MAMP addition and 30 and 60 minutes after MAMP addition. Total RNA was isolated using the RNeasy Plant Kit (QIAGEN, Hilden, Germany). cDNA was synthesized with 5 µg total RNA, oligo dT primers and Superscript II reverse transcriptase (Invitrogen, Karlsruhe, Germany) according to manufacturers protocol. Transcript abundance was quantified using the IQ5 real-time PCR thermocycler (Bio-Rad, Munich, Germany). The expression of the genes of interest was normalized to *At4g26410* (for primers used see [27]) and to the relative transcript abundance in non-treated Col-0 control samples as calculated according to the comparative cycle threshold (ΔΔCt) method [28]. Transcript abundance of a MAPK dependent gene, *FRK1* and a CDPK dependent gene, *PHI-1,* were tested (for primers used see [29]). Three biological replicates with three technical replicates per sample were performed per treatment.

Results

MAMP-triggered Ca^{2+} influx from the apoplast

We used the luminescent aequorin Ca^{2+} sensor system [24] to record whole seedling intracellular Ca^{2+} transients in response to MAMPs. Owing to previous in-depth characterization and the identification of the cognate PRRs we focused on responses towards the bacterial peptide elicitors flg22 and elf18 [2, 3] as well as chitin, a carbohydrate polymer that represents the major constituent of fungal cell walls [30]. To narrow down candidate protein classes involved in regulating MAMP-triggered Ca^{2+} signatures in *Arabidopsis*, a range of chemicals were chosen that are known to target components controlling Ca^{2+} in- and efflux in plant and animal systems. Due to potential plant off-targets, presumed differences in bioavailability, compound metabolism and dissimilarities in the molecular structure of plant and animal targets we generally tested multiple chemicals affecting the same molecule class.

To investigate the source of the initial intracellular [Ca^{2+}] rise, the general Ca^{2+} channel inhibitor Lanthanum chloride ($LaCl_3$) and a chelator of extracellular bivalent cations, ethylene glycol-bis(2-aminoethylether)-N,N,N′,N′-tetraacetic acid (EGTA), were applied. Consistent with previous reports [6, 31] flg22 and elf18 induced a biphasic Ca^{2+} response with a maximum [Ca^{2+}] at about three minutes after MAMP addition and a recovery phase of ca. 20-30 minutes (Figures 1A and 1B). Chitin induced a monophasic Ca^{2+} transient (Figure 1C). Preincubation of the seedlings with either $LaCl_3$ or EGTA fully inhibited the Ca^{2+} transients induced by all three MAMPs, suggesting the main Ca^{2+} source for the MAMP-triggered spikes is the apoplast (Figures 1, A-D, Supplemental Figures S1A and B and Table 1). In the presence of EGTA, a continuous rise in intracellular Ca^{2+} levels was observed, independent of the presence or absence of MAMPs (Figure 1D, Supplemental Figure S1A and B).

An ambiguous role for internal Ca^{2+} stores in MAMP-triggered Ca^{2+} influx

To further validate the conclusion that the major source of MAMP-induced Ca^{2+} is the apoplast we studied the role of phospholipase C (PLC)-dependent release of Ca^{2+} from intracellular stores using the PLC inhibitors neomycin and U73122 [32, 33]. Both inhibitors led to increased steady state Ca^{2+} levels (Figure 2A, Supplemental Figure S2C and Table 1). U73122 did not alter Δ[Ca^{2+}] for the tested MAMPs, but changed the shape of the response curves of elf18 and chitin (Figure 2B, Supplemental Figures S2A and B), which suggests a minor contribution for PLC-controlled Ca^{2+} release in response to these MAMPs. Neomycin did not alter the chitin-induced Δ[Ca^{2+}] (Supplemental Figure S2F), but caused a slight reduction in the flg22- and elf18-induced Δ[Ca^{2+}] (Supplemental Figures S2C-E). In

conclusion, PLC-mediated Ca^{2+} release has a minor, if any, contribution to the MAMP-triggered $\Delta[Ca^{2+}]$.

A MAMP-triggered primary apoplastic Ca^{2+} influx does not exclude the possibility of secondary Ca^{2+}-induced Ca^{2+} release (CICR) from internal stores. Ruthenium Red (RR) inhibits CICR from internal stores in plant and animal systems [34], but also inhibits certain channels at the plasma membrane [35, 36]. Like inhibition of the PLC pathway, addition of RR resulted in increased steady state $[Ca^{2+}]$ (Supplemental Figure S2G and Table 1). In addition, the chitin- and elf18-triggered $\Delta[Ca^{2+}]$ were strongly reduced compared to the uninhibited situation (Figures 2C and D), while the flg22-induced $\Delta[Ca^{2+}]$ was largely unaffected (Supplemental Figures S2G and H). This suggests either a significant contribution of CICR from intracellular stores or, alternatively, a role for specific RR-targeted plasma membrane-localized channels in the chitin and elf18 responses. Like RR, tetracaine directly targets mammalian ryanodine receptors and blocks CICR from intracellular stores [34]. Tetracaine induced a higher $\Delta[Ca^{2+}]$ for all three MAMPs and interfered with the recovery phase, visible as irregular spikes during the decline of the Ca^{2+} response (Figure 2E, Supplemental Figures S2I-J and Table 1). Unlike for the other intracellular store channel inhibitors, in the case of tetracaine no increased steady state $[Ca^{2+}]$ was observed (not shown). In sum, the compounds targeting internal Ca^{2+} stores yielded ambiguous data. A role for PLC-dependent Ca^{2+} release and /or CICR in response to MAMP treatment can thus not be ruled out.

Inhibitors of voltage- and nucleotide-gated channels do not affect MAMP-triggered Ca^{2+} influx

To further delimit the channels involved in Ca^{2+} import from extracellular stores, a set of inhibitors targeting animal type voltage-gated Ca^{2+} channels (VGCC) were tested. Although plants lack obvious candidate genes coding for VGCCs, electrophysiological data support their existence in plant organelles and cells [11, 12]. None of the three L-type VGCC inhibitors, verapamil, diltiazem and nifedipine, altered the $\Delta[Ca^{2+}]$ after MAMP stimulus (Figure 2F and Supplemental Figures S3A-H and Table 1). Nifedipine treatment resulted in a delayed recovery in the case of all three MAMPs (Figure 2F and Supplemental Figures S3A-B and Table 1). Verapamil-treated seedlings occasionally showed random spiking after the MAMP stimulus (Supplemental Figures S3C–E and Table 1). Together, these results suggest that the sensing of flg22, elf18 or chitin does not activate Ca^{2+} influx through VGCCs.

Plant genomes encode two major classes of putative Ca^{2+} channels, CNGCs and iGluRs. Two compounds were tested that interfere with cNTP biosynthesis and therefore indirectly inhibit CNGC function, alloxan and dideoxyadenosine (DDA). Neither incubation of seedlings with alloxan nor treatment with DDA caused an alteration of the MAMP-induced $\Delta[Ca^{2+}]$ for flg22 (Figures 3A and B, Supplemental Figure S5C and Table 1). For elf18 and chitin the $\Delta[Ca^{2+}]$ was slightly lower in the presence of alloxan or DDA (Supplemental Figures S4A-D, Supplemental Figures S5F and I and Table 1) DDA pretreatment resulted in a delayed recovery of cellular Ca^{2+} levels after MAMP stimulation (Figure 3B, Supplemental Figures S4C and D and Table 1). These results suggest that, dissimilar to lipopolysaccharides (LPS) [13] cyclic nucleotide biosynthesis and thus likely also CNGCs do not make a major contribution to the flg22-, elf18- or chitin-induced Ca^{2+} influx.

Inhibition of iGluR-like channels affects MAMP-triggered Ca^{2+} influx

The second major class of putative Ca^{2+} channels in plants comprises the iGluR-like channels, which include 20 members in *Arabidopsis* [9, 10, 19]. We employed various inhibitors directed against NMDA- and non-NMDA-like mammalian iGluRs. AP-5 and AP-7, competitive antagonists of the glutamate binding site [37] and kynurenic acid, a competitive antagonist of the glycine binding site [38], caused a strong inhibition of the MAMP-triggered $\Delta[Ca^{2+}]$. For all three MAMPs, the reduction induced by both AP-5 and kynurenic acid was statistically significant ($p<0,05$). Treatment with these inhibitors also led to increased steady state $[Ca^{2+}]$ (Figures 4A-C, Supplemental Figures S4E-H and Table 1). The observation that increased cellular Ca^{2+} concentrations in the presence of U73122 still allowed a normal flg22-, elf18- and chitin-induced $\Delta[Ca^{2+}]$ (Figures 2A and B, Supplemental Figures S2A and B) suggests that elevated steady state Ca^{2+} levels do not per se impede a MAMP-triggered Ca^{2+} transient. Other iGluR channel inhibitors tested targeting either the channel domain of NMDA-like channels (MK-801) [37] or non-NMDA iGluR channels (DNQX, CNQX) [39] did not inhibit MAMP-triggered $\Delta[Ca^{2+}]$ (Supplemental Figure S6 and Table 1). Together, these data provide first

evidence for a potential role of iGluR-like channels in the generation of the flg22-, elf18- and chitin-triggered Ca^{2+} transient.

To further analyze the potential role of iGluRs in MAMP-induced Ca^{2+} influx, we exploited the phenomenon of iGluR desensitization [40]. If iGluRs were the channels mediating MAMP-triggered Ca^{2+} influx, then agonistic amino acids such as L-glutamate and L-aspartate should desensitize the channels for subsequent MAMP treatment, while other amino acids should have either less or no effect. We thus monitored the MAMP-triggered Ca^{2+} response after preincubation of the aequorin-expressing seedlings with ten different amino acids that differ largely in their physiochemical properties (Figure 4F). Pretreatment of seedlings with both L-glutamate and L-aspartate resulted in a statistically significant reduction ($p<0,05$) of the $\Delta[Ca^{2+}]$ after flg22 stimulation (Figures 4D-E, Supplemental Figures S4I-J and Table 1). In addition, reminiscent of treatment with the inhibitors AP-5, AP-7 and kynurenic acid, basal cellular $[Ca^{2+}]$ levels were elevated to 125%-158% of the control following application of these two negatively charged amino acids (Figure 4D and F and Table 1). Other amino acids did neither reduce the MAMP-induced $\Delta[Ca^{2+}]$ nor affect basal cellular $[Ca^{2+}]$ (Figure 4F).

We then tested a range of L-glutamate concentrations for desensitization of the flg22-mediated Ca^{2+} transient and established a dose-response curve (Figure 4G). We found a concentration-dependent reduction of $\Delta[Ca^{2+}]$ and a reciprocal concentration-dependent increase in steady state Ca^{2+} levels. From a concentration of 0,2 mM L-glutamate onwards a reduction of $\Delta[Ca^{2+}]$ and an increase in basal cellular $[Ca^{2+}]$ was observed. Pretreatment with concentrations above 0,6 mM L-glutamate resulted in maximal inhibition of the flg22-triggered Ca^{2+} transient, indicating saturation of the system (Figure 4G). The concentration range where L-glutamate desensitized MAMP-induced Ca^{2+} influx is in agreement with the reported K_m values for plant iGluR-like channels, which were found to be between 0,2 and 0,5 mM [41], similar to reported apoplastic amino acid concentrations (0,3-1,3 mM) [42, 43]. In sum, the results of desensitization experiments further support a role of iGluRs in MAMP-triggered Ca^{2+} influx.

iGluR inhibitors and L-glutamate modulate MAMP-induced MAPK activation

To expand the analysis of cellular responses induced by compounds that affect iGluR activity, we inspected other early MAMP-triggered events. Upon biotic stress specific MAPK signaling cascades are activated, which control additional cellular responses and defense gene expression [44]. We examined MAMP-induced MAPK activation in the presence or absence of L-glutamate or the iGluR inhibitors kynurenic acid or CNQX. Application of L-glutamate as a stimulus to seedlings resulted in low levels of MAPK activation, visible as three additional bands (MPK6, MPK3 and MPK4) appearing at five minutes after addition of L-glutamate or the MAMP stimulus (Figure 5A). Preincubation with either L-glutamate or kynurenic acid for one hour resulted in low levels of MAPK activation. Subsequent addition of more L-glutamate still transiently increased activated MAPK levels. Preincubation of the seedlings with CNQX, which did not affect the MAMP-triggered Ca^{2+} signature, completely abolished MAPK activation after L-glutamate addition (Figure 5A).

Flg22, elf18 and chitin induced strong MAPK activation within 5 minutes after MAMP addition (Figures 5B and C and Supplemental Figure S7). In the presence of L-glutamate, kynurenic acid or CNQX, the flg22 and elf18 response was only affected to a minor extent. The presence of L-glutamate or kynurenic acid often delayed MAPK activation, with full activation not before 15 minutes (Supplemental Figure S7). In contrast, all three compounds markedly reduced the chitin-triggered activation of the MAPK(K/KK) cascade (Figure 5B).

Recently, Boudsocq and co-workers [29] showed that flg22-induced MAPK activation in *Arabidopsis* protoplasts does not depend, but is enhanced by Ca^{2+} influx. To corroborate this observation in intact *Arabidopsis* seedlings and to compare it with the glutamate-dependent inhibition of MAPK activation, we performed MAPK assays in the presence of either EGTA or $LaCl_3$. In the case of flg22, full MAPK activation was delayed by both EGTA and $LaCl_3$ (Supplemental Figure S7B). In the case of elf18 and chitin, EGTA reduced and $LaCl_3$ delayed MAPK activation (Figure 5C and Supplemental Figure S7D). In conclusion, MAMP-triggered MAPK signaling requires Ca^{2+} influx for full and timely activation. Modulation of MAMP-triggered Ca^{2+} influx by iGluR inhibitors or glutamate desensitization affected MAPK activation in a similar manner as full inhibition (Figures 1A-D) of apoplastic Ca^{2+} influx by the potent non-selective chemicals $LaCl_3$ and EGTA.

Cooperative regulation of Ca^{2+} influx by CNGC and iGluR-like channels?
Modulating glutamate-controlled Ca^{2+} influx did largely but not fully abolish the MAMP-triggered Ca^{2+} transient (Figure 4; Supplemental Figures S4 and S5). Therefore we wondered if cNTP-regulated Ca^{2+} import was responsible for the remaining influx of Ca^{2+} and possibly a positive feedback loop exists between both channel types. Plants were co-treated with both kynurenic acid/L-glutamate and alloxan/dideoxyadenosine before MAMP addition and both Ca^{2+} levels and MAPK activation were followed. For elf18, but not for flg22 and chitin, the combined incubations gave a stronger reduction in $\Delta[Ca^{2+}]$ than each of the single compounds (compare Figure 6A with Supplemental Figures S8A and C, Table 1). As discussed above, L-glutamate pretreatment reduced (chitin) or delayed (flg22 and elf18) MAPK activation. Alloxan pretreatment did not influence the intensity of the two major MAPK bands (MPK6 and MPK3), but reduced the intensity of the MAPK band with the highest electrophoretic mobility, which likely represents MPK4 (Figure 6B and Supplemental Figures S8B and D). The co-inhibition of cNTP- and iGluR-mediated Ca^{2+} influx resulted in a combination of both effects; the major MAPK bands representing MPK3 and 6 showed a delayed activation (elf18) or reduced intensity (chitin) and nearly no activation of MPK4 could be detected anymore (Figure 6B and Supplemental Figures S8B, D and F). In conclusion, we did not find evidence for a strong cooperative effect of iGluR-like channels and CNGCs in MAMP-triggered Ca^{2+} influx.

Glutamate signaling differentially modulates MAPK- and CDPK-dependent defense gene transcript levels in response to MAMPs
To investigate how the modulation of iGluR-like channels impacts on MAMP-triggered transcriptional activation of defense genes, we studied transcript accumulation of each a MAPK- and a CDPK-dependent gene (*FLG22-INDUCED-RECEPTOR-LIKE-KINASE1, FRK1,* and *PHOSPHATE-INDUCED1, PHI-1,* respectively) [29] using quantitative RT-PCR. *FRK1* transcript accumulation was rapidly (within 30 minutes) induced by each of the three MAMPs (Figure 7A). Application of either L-glutamate or kynurenic acid reduced basal *FRK1* expression levels and drastically impaired MAMP-dependent accumulation of *FRK1* transcripts (Figure 7A). *PHI-1* transcript levels were strongly and transiently induced by flg22 and moderately by elf18 or chitin (Figure 7B). L-glutamate and kynurenic acid each increased basal *PHI-1* expression levels and blocked an additional increase in transcript accumulation upon MAMP treatment. Thus, modulation of MAMP-triggered Ca^{2+} influx by L-glutamate or kynurenic acid inhibits transcriptional up-regulation of genes downstream of the MAPK (*FRK1*) and CDPK (*PHI-1*) signaling cascades.

Discussion

We tested a comprehensive set of compounds known to target various components regulating Ca^{2+} signaling for their influence on MAMP-induced Ca^{2+} influx in *Arabidopsis* seedlings. Pharmacological approaches bear the risk of unspecific off-targets, but offer the advantage to overcome potential redundancy in target function and allow transient inhibition with minimal pleiotropic effects. We opted for a pharmacological approach to surmount the presumed genetic redundancy of plant Ca^{2+} channels and the expected pleiotropic phenotypes of respective mutants. We aimed to minimize the impact of off-targets on our data by applying multiple inhibitors per target molecule class in most cases.

Inhibition of iGluR-like channels affects MAMP-triggered Ca^{2+} influx
Flg22 and elf18 induced biphasic Ca^{2+} transients that were very similar in shape and timing, while chitin caused a monophasic Ca^{2+} transient (e.g. Figure 1A and C). The presence of two separate maxima in the case of flg22 and elf18 suggests either the involvement of different channel types, different subcellular Ca^{2+}-stores or a differential responsiveness between cell types. The aequorin reporter system used in this study does not allow the detection of changes in $[Ca^{2+}]$ at the (sub)cellular level. Therefore, other reporters like the yellow cameleon FRET sensor are desirable for future analyses with improved spatial resolution [46, 47].

$LaCl_3$-mediated inhibition of plasma membrane-resident ion channels and chelating external Ca^{2+} via EGTA treatment revealed that the primary Ca^{2+} pool for both types of MAMP-triggered Ca^{2+}-signatures is the apoplast (Figures 1A-D and Supplemental Figures S1A-C). This confirms and extends findings of a previous study [45], where $LaCl_3$ was used to demonstrate that flg22-induced Ca^{2+} influx is needed for membrane depolarization in mesophyll cells. Furthermore, both inhibition of Ca^{2+} influx by $LaCl_3$ and chelating apoplastic Ca^{2+} were shown to prevent CDPK activation and to reduce MAPK activation in response to the peptide elicitors flg22 and elf18 in *Arabidopsis* protoplasts [29]. These findings suggest a role for Ca^{2+} signaling in modulating downstream responses during MAMP-triggered immunity.

Interference with $InsP_3$ or CICR resulted in increased steady state Ca^{2+} levels for three of the inhibitors tested (U73122, Neomycin and RR). Notably, although basal Ca^{2+} levels were increased, a normal Ca^{2+} transient was induced (Figures 2A-B). In addition, RR reduced the chitin- and elf18-induced Ca^{2+} transients, possibly due its inhibitory effect on plasma membrane-resident ion channels[35, 36]. The fourth compound, tetracaine, caused a slightly enhanced Ca^{2+} transient, but did not alter basal Ca^{2+} levels.

Inhibition of VGCCs did not change the intensity of MAMP-triggered Ca^{2+} transients, but for two inhibitors (verapamil and nifedipine) delayed the recovery to basal cytosolic Ca^{2+} levels (Figure 2F and Supplemental Figure S3). VGCC inhibitors have documented effects in plants [35, 48]. However, all three L-type channel inhibitors have also other reported targets than L-type Ca^{2+} channels, including sodium channels and membrane receptors (https://www.ebi.ac.uk/chembldb/). The prolonged Ca^{2+} signature might thus be due to interference with other ion channel types and a resulting altered recovery of the membrane potential or ion gradients including Ca^{2+}.

Inhibitors of CNGCs previously shown to inhibit CNGC-mediated responses *in planta* [13], DDA and alloxan, caused only a slight reduction in the MAMP-triggered Ca^{2+} transients. Therefore in contrast to LPS [13] and the Danger-Associated Molecular Pattern (DAMP) AtPep3 [14], cNTPs and thus likely CNGCs do not control the flg22-, elf18- and chitin-induced Ca^{2+} transient. *cngc2* mutants lose the LPS-induced Ca^{2+} increase [13], but show normal flg22-triggered membrane depolarization [45]. It appears that the MAMPs used in the present study activate a different set of ion channels than LPS does. The proposed discrepancy between the channels involved is in line with the different gene sets activated by the two groups of elicitors [29]. Surprisingly, the flg22-induced Ca^{2+} transient is attenuated in a *Atpepr1* mutant background [14], which suggests crosstalk at the level of Ca^{2+} influx between the AtPep and flg22/elf18/chitin pathways independent of cNTP generation. The delayed recovery of the MAMP-induced cytosolic rise in Ca^{2+} levels in the presence of DDA suggests a role for cNTPs in controlling Ca^{2+} efflux.

Of the six iGluR inhibitors tested, AP-5, AP-7 and kynurenic acid resulted in a strong reduction in the MAMP-induced $\Delta[Ca^{2+}]$ and all three led to an increase in cytosolic $[Ca^{2+}]$ (Figures 4A-C , Supplemental Figures S4-6 and Table 1 and 2). MK-801, CNQX and DNQX pretreatment did not alter flg22-, elf18- or chitin-induced Ca^{2+} fluxes (Supplemental Figure S6). AP-5, CNQX and DNQX have been previously shown to affect iGluR-mediated processes and Ca^{2+} currents in pollen tube growth (AP-5, CNQX, DNQX) [21], hypocotyl elongation (DNQX)[22], glutamate-induced Ca^{2+} transients in mesophyll cells (CNQX, DNQX)[20] and responses to Al^{3+}-induced Ca^{2+} transients in roots (AP-5) [48]. Most recently, AP-5 was found to strongly inhibit Ca^{2+} influx induced by the peptide elicitor cryptogein in tobacco cell culture, while MK-801 and DNQX were significantly less effective in these experiments [23]. Based on these published findings, a subset of the iGluR inhibitors can efficiently modulate both NMDA- and non-NMDA-like iGluR channels. In our hands, DNQX, CNQX and MK-801 did not result in inhibition of MAMP-induced Ca^{2+} influx (Supplemental Figure S6). Possibly these compounds were unstable in our experimental conditions or were unable to penetrate the seedling tissue well enough to compete with glutamate for binding sites. In pollen tubes, AP-5 had a stronger influence on Ca^{2+} currents than CNQX and DNQX, suggesting that higher apoplastic concentrations of the latter compounds are needed [21], which might not have been achieved in our experimental set-up. Alternatively, various plant iGluR channels or iGluR channel complexes may differ in their sensitivity towards the inhibitors. The channel domain of some plant iGluR-like channels are permeable to Ca^{2+}, Na^+ and K^+ [18], but they differ in conserved amino acids controlling channel selectivity from animal iGluRs [18, 19], which might explain the inactivity of MK-801 in our experiments. Interestingly, inhibitor treatment and de-sensitization of the MAMP responses with L-

glutamate or L-aspartate resulted in similar changes of the Ca^{2+} response and increased steady state [Ca^{2+}] (Figure 4, Table 1 and 2). The increased steady state Ca^{2+} levels in the presence of both inhibitors and agonists can be best rationalized by either an unexpected partial agonistic function of the presumed inhibitors or by hyper-compensation of interference with iGluR-like channel function via other Ca^{2+} channel types.

Inhibition of iGluR-like channel does not fully abolish the Ca^{2+} spike, which suggests either partial inhibition of these channels or the involvement of a second channel class in the response. A second channel class acting in the flg22- and elf18-mediated Ca^{2+} influx would explain the biphasic shape of the Ca^{2+} response for these MAMPs. However, chitin-induced fluxes are altered in a similar manner, which argues for an alternative explanation of the phenomenon. Our experiments suggest the potential second class of channels is not cNTP-activated, since co-treatment with inhibitors of adenylate cyclases and iGluRs did not fully block Ca^{2+} influx (Figure 6A).

We exploited the phenomenon of iGluR channel desensitization by analyzing the MAMP response after pretreatment with various amino acids. In our experiments, flg22-, elf18- and chitin-induced responses were only desensitized by the negatively charged L-glutamate and L-aspartate (Figures 4D-G, Supplemental Figures S4I and J). In a previous study certain combinations of amino acids were tested for cross-desensitization and the dependence on the presence of AtGLR3.3 and AtGLR3.4 [40]. The results of this work fit a model where various quaternary complexes of iGluR-like channels co-exist that vary in their sensitivity to different amino acids. Taking this model into account, the iGluR complex(es) activated by MAMPs only seem(s) to contain subunits sensitive to both L-glutamate and L-aspartate. Comparative modeling of the glutamate binding site of plant iGluR-like channels suggested that only AtGLR1.1 can bind glutamate, while the other family members bind glycine [22]. This suggests that the iGluR complex responsible for MAMP- triggered Ca^{2+} influx would have to contain AtGLR1.1. However, modeling studies alone are insufficient to exclude binding of other amino acids [49]. Furthermore, L-glutamate or L-aspartate might not directly bind the receptor, but induce the release of another compound that modulates iGluR-like channel activity [49].

iGluR-mediated Ca^{2+} influx controls defense gene expression

Reduction of MAMP-triggered Ca^{2+} influx fully inhibited expression of a MAPK-dependent gene (*FRK1*) and increased steady state levels of a CDPK-dependent gene (*PHI-1*) (Figure 7) [29]. Given the only modest effect of L-glutamate und kynurenic acid on MAPK activation (Figure 5 and Supplemental Figure S7) the strong impact on MAPK-dependent *FRK1* expression was surprising. This result suggests that either the signal transduction cascade leading from Ca^{2+} influx to the activation of *FRK1* transcript accumulation relies only partially on MAPK activation, or that a moderate impact on MAPK activity can have a profound effect on downstream gene expression. The enhanced steady state *PHI-1* transcript levels seen upon treatment with L-glutamate or kynurenic acid are possibly a consequence of the enhanced intracellular steady state Ca^{2+} levels caused by these compounds, which may lead to constitutive low level activation of CDPKs. Notably, a further MAMP-induced increase in *PHI-1* transcript levels was also blocked by L-glutamate and kynurenic acid. In sum, these data indicate a crucial role for cellular signaling events upon MAMP perception that rely on iGluR-mediated Ca^{2+} influx. It remains to be seen to what extent the reduction in defense gene activation translates into a compromised immune response. In this context it would be highly desirable to examine the effect of interference with Ca^{2+} signaling during authentic plant-microbe interactions. However, the dual effect of compounds on both the host and the parasite combined with the resulting complication in interpreting the data from such experiments emphasize the limitations of pharmacological approaches.

A model for iGluR-mediated Ca^{2+} influx

Based on our data we propose the following model for MAMP-triggered Ca^{2+} influx (Figure 8): Following MAMP perception by cognate PRRs, glutamate-dependent opening of iGluR-like channels and Ca^{2+} influx from the apoplast into the cytoplasm is activated by yet unknown mechanisms. This may involve vesicle-mediated secretion of L-glutamate into the apoplast [23]. Elevated cytoplasmic Ca^{2+} levels translate via CDPK- and MAPK-dependent pathways into defense gene activation. It remains unclear how Ca^{2+} influx via iGluRs is terminated. One possibility is a negative feedback loop that involves Ca^{2+}-dependent calmodulin (CaM) binding to hypothetical CaM binding domain(s) of

iGluR-like channels. As a next step, reverse genetic approaches are required to further substantiate the findings of the present study at a different experimental level. In our hands the analysis of a subset of iGluR single mutants did not yet result in the identification of mutants that exhibit altered MAMP-induced Ca^{2+} signatures. These preliminary data indeed argue for redundant iGluR functions in plant innate immunity.

Acknowledgements
We thank Justine Lorek for providing protocols and primer sequences for qRT-PCR and MAPK assays. We are grateful to the lab of Tina Romeis for performing CDPK activity assays. We acknowledge Dierk Scheel and Mark Knight for kindly providing seeds of the 35S-aequorin line. We apologize to authors whose work could not be cited due to space constraints.

Funding
Work in the lab of RP is supported by grants from the Max-Planck society and the Deutsche Forschungsgemeinschaft (DFG; SFB670).

References

1 Boller, T. and Felix, G. (2009) A renaissance of elicitors: perception of microbe-associated molecular patterns and danger signals by pattern-recognition receptors. Annu. Rev. Plant Biol. **60**, 379-406

2 Gómez-Gómez, L. and Boller, T. (2000) FLS2: an LRR receptor-like kinase involved in the perception of the bacterial elicitor flagellin in *Arabidopsis*. Mol. Cell **5**, 1003-1011

3 Zipfel, C., Kunze, G., Chinchilla, D., Caniard, A., Jones, J. D., Boller, T. and Felix, G. (2006) Perception of the bacterial PAMP EF-Tu by the receptor EFR restricts *Agrobacterium*-mediated transformation. Cell **125**, 749-760

4 Miya, A., Albert, P., Shinya, T., Desaki, Y., Ichimura, K., Shirasu, K., Narusaka, Y., Kawakami, N., Kaku, H. and Shibuya, N. (2007) CERK1, a LysM receptor kinase, is essential for chitin elicitor signaling in *Arabidopsis*. Proc. Natl. Acad. Sci. U.S.A. **104**, 19613-19618

5 Lecourieux, D., Ranjeva, R. and Pugin, A. (2006) Calcium in plant defence-signalling pathways. New Phytol. **171**, 249-269

6 Aslam, S. N., Erbs, G., Morrissey, K. L., Newman, M. A., Chinchilla, D., Boller, T., Molinaro, A., Jackson, R. W. and Cooper, R. M. (2009) Microbe-associated molecular pattern (MAMP) signatures, synergy, size and charge: influences on perception or mobility and host defence responses. Mol. Plant Pathol. **10**, 375-387

7 Bush, D. S. (1995) Calcium regulation in plant cells and its role in signaling. Annu. Rev. Plant Physiol. Plant Mol. Biol. **46**, 95-122

8 Mäser, P., Thomine, S., Schroeder, J. I., Ward, J. M., Hirschi, K., Sze, H., Talke, I. N., Amtmann, A., Maathuis, F. J., Sanders, D., Harper, J. F., Tchieu, J., Gribskov, M., Persans, M. W., Salt, D. E., Kim, S. A. and Guerinot, M. L. (2001) Phylogenetic relationships within cation transporter families of Arabidopsis. Plant Physiol. **126**, 1646-1667

9 Wheeler, G. L. and Brownlee, C. (2008) Ca^{2+} signalling in plants and green algae - changing channels. Trends Plant Sci. **13**, 506-514

10 Chiu, J. C., Brenner, E. D., DeSalle, R., Nitabach, M. N., Holmes, T. C. and Coruzzi, G. M. (2002) Phylogenetic and expression analysis of the glutamate-receptor-like gene family in *Arabidopsis thaliana*. Mol. Biol. Evol. **19**, 1066-1082

11 Demidchik, V., Bowen, H. C., Maathuis, F. J., Shabala, S. N., Tester, M. A., White, P. J. and Davies, J. M. (2002) *Arabidopsis thaliana* root non-selective cation channels mediate calcium uptake and are involved in growth. Plant J. **32**, 799-808

12 Miedema, H., Demidchik, V., Very, A. A., Bothwell, J. H., Brownlee, C. and Davies, J. M. (2008) Two voltage-dependent calcium channels co-exist in the apical plasma membrane of *Arabidopsis thaliana* root hairs. New Phytol. **179**, 378-385

13 Ma, W., Qi, Z., Smigel, A., Walker, R. K., Verma, R. and Berkowitz, G. A. (2009) Ca^{2+}, cAMP, and transduction of non-self perception during plant immune responses. Proc. Natl. Acad. Sci. U.S.A. **106**, 20995-21000

14 Qi, Z., Verma, R., Gehring, C., Yamaguchi, Y., Zhao, Y., Ryan, C. A. and Berkowitz, G. A. (2010) Ca^{2+} signaling by plant *Arabidopsis thaliana* Pep peptides depends on AtPepR1, a receptor with guanylyl cyclase activity, and cGMP-activated Ca^{2+} channels. Proc. Natl. Acad. Sci. U.S.A. **107**, 21193-21198

15 Clough, S. J., Fengler, K. A., Yu, I. C., Lippok, B., Smith, R. K., Jr. and Bent, A. F. (2000) The *Arabidopsis dnd1* "defense, no death" gene encodes a mutated cyclic nucleotide-gated ion channel. Proc. Natl. Acad. Sci. U.S.A. **97**, 9323-9328

16 Jurkowski, G. I., Smith, R. K., Jr., Yu, I. C., Ham, J. H., Sharma, S. B., Klessig, D. F., Fengler, K. A. and Bent, A. F. (2004) *Arabidopsis DND2*, a second cyclic nucleotide-gated ion channel gene for which mutation causes the "*defense, no death*" phenotype. Mol. Plant-Microbe Interact. **17**, 511-520

17 Tikhonov, D. B. and Magazanik, L. G. (2009) Origin and molecular evolution of ionotropic glutamate receptors. Neurosci. Behav. Physiol. **39**, 763-773
18 Tapken, D. and Hollmann, M. (2008) *Arabidopsis thaliana* glutamate receptor ion channel function demonstrated by ion pore transplantation. J. Mol. Biol. **383**, 36-48
19 Chiu, J., DeSalle, R., Lam, H. M., Meisel, L. and Coruzzi, G. (1999) Molecular evolution of glutamate receptors: a primitive signaling mechanism that existed before plants and animals diverged. Mol. Biol. Evol. **16**, 826-838
20 Meyerhoff, O., Müller, K., Roelfsema, M. R., Latz, A., Lacombe, B., Hedrich, R., Dietrich, P. and Becker, D. (2005) *AtGLR3.4*, a glutamate receptor channel-like gene is sensitive to touch and cold. Planta **222**, 418-427
21 Michard, E., Lima, P. T., Borges, F., Silva, A. C., Portes, M. T., Carvalho, J. E., Gilliham, M., Liu, L. H., Obermeyer, G. and Feijo, J. A. (2011) Glutamate receptor-like genes form Ca^{2+} channels in pollen tubes and are regulated by pistil D-serine. Science **332**, 434-437
22 Dubos, C., Huggins, D., Grant, G. H., Knight, M. R. and Campbell, M. M. (2003) A role for glycine in the gating of plant NMDA-like receptors. Plant J. **35**, 800-810
23 Vatsa, P., Chiltz, A., Bourque, S., Wendehenne, D., Garcia-Brugger, A. and Pugin, A. (in press) Involvement of putative glutamate receptors in plant defence signaling and NO production. Biochimie (in press)
24 Knight, M. R., Campbell, A. K., Smith, S. M. and Trewavas, A. J. (1991) Transgenic plant aequorin reports the effects of touch and cold-shock and elicitors on cytoplasmic calcium. Nature **352**, 524-526
25 Rentel, M. C. and Knight, M. R. (2004) Oxidative stress-induced calcium signaling in Arabidopsis. Plant Physiol. **135**, 1471-1479
26 Saijo, Y., Tintor, N., Lu, X., Rauf, P., Pajerowska-Mukhtar, K., Haweker, H., Dong, X., Robatzek, S. and Schulze-Lefert, P. (2009) Receptor quality control in the endoplasmic reticulum for plant innate immunity. EMBO J. **28**, 3439-3449
27 Czechowski, T., Stitt, M., Altmann, T., Udvardi, M. K. and Scheible, W. R. (2005) Genome-wide identification and testing of superior reference genes for transcript normalization in Arabidopsis. Plant Physiol. **139**, 5-17
28 Libault, M., Wan, J., Czechowski, T., Udvardi, M. and Stacey, G. (2007) Identification of 118 *Arabidopsis* transcription factor and 30 ubiquitin-ligase genes responding to chitin, a plant-defense elicitor. Mol. Plant-Microbe Interact. **20**, 900-911
29 Boudsocq, M., Willmann, M. R., McCormack, M., Lee, H., Shan, L., He, P., Bush, J., Cheng, S. H. and Sheen, J. (2010) Differential innate immune signalling via Ca^{2+} sensor protein kinases. Nature **464**, 418-422
30 Felix, G., Regenass, M. and Boller, T. (1993) Specific perception of subnanomolar concentrations of chitin fragments by tomato cells: induction of extracellular alkalinization, changes in protein-phosphorylation, and establishment of a refractory state. Plant J. **4**, 307-316
31 Lecourieux, D., Lamotte, O., Bourque, S., Wendehenne, D., Mazars, C., Ranjeva, R. and Pugin, A. (2005) Proteinaceous and oligosaccharidic elicitors induce different calcium signatures in the nucleus of tobacco cells. Cell Calcium **38**, 527-538
32 de Jong, C. F., Laxalt, A. M., Bargmann, B. O., de Wit, P. J., Joosten, M. H. and Munnik, T. (2004) Phosphatidic acid accumulation is an early response in the *Cf-4*/*Avr4* interaction. Plant J. **39**, 1-12
33 Munnik, T. and Testerink, C. (2009) Plant phospholipid signaling: "in a nutshell". J. Lipid Res. **50 Suppl**, S260-265
34 Endo, M. (2009) Calcium-induced calcium release in skeletal muscle. Physiol. Rev. **89**, 1153-1176

35 Pineros, M. and Tester, M. (1997) Calcium channels in higher plant cells: selectivity, regulation and pharmacology. J. Exp. Bot. **48**, 551-577
36 Pottosin, II, Dobrovinskaya, O. R. and Muniz, J. (1999) Cooperative block of the plant endomembrane ion channel by ruthenium red. Biophys. J. **77**, 1973-1979
37 Foster, A. C. and Wong, E. H. (1987) The novel anticonvulsant MK-801 binds to the activated state of the N-methyl-D-aspartate receptor in rat brain. Brit. J. Pharmacol. **91**, 403-409
38 Bertolino, M., Vicini, S. and Costa, E. (1989) Kynurenic acid inhibits the activation of kainic and N-methyl-D-aspartic acid-sensitive ionotropic receptors by a different mechanism. Neuropharmacology **28**, 453-457
39 Honore, T., Davies, S. N., Drejer, J., Fletcher, E. J., Jacobsen, P., Lodge, D. and Nielsen, F. E. (1988) Quinoxalinediones: potent competitive non-NMDA glutamate receptor antagonists. Science **241**, 701-703
40 Stephens, N. R., Qi, Z. and Spalding, E. P. (2008) Glutamate receptor subtypes evidenced by differences in desensitization and dependence on the *GLR3.3* and *GLR3.4* genes. Plant Physiol. **146**, 529-538
41 Demidchik, V., Essah, P. A. and Tester, M. (2004) Glutamate activates cation currents in the plasma membrane of *Arabidopsis* root cells. Planta **219**, 167-175
42 Lohaus, G., Pennewiss, K., Sattelmacher, B., Hussmann, M. and Hermann Muehling, K. (2001) Is the infiltration-centrifugation technique appropriate for the isolation of apoplastic fluid? A critical evaluation with different plant species. Physiol. Plant. **111**, 457-465
43 Forde, B. G. and Lea, P. J. (2007) Glutamate in plants: metabolism, regulation, and signalling. J. Exp. Bot. **58**, 2339-2358
44 Pitzschke, A., Schikora, A. and Hirt, H. (2009) MAPK cascade signalling networks in plant defence. Curr. Opin. Plant Biol. **12**, 421-426
45 Jeworutzki, E., Roelfsema, M. R., Anschütz, U., Krol, E., Elzenga, J. T., Felix, G., Boller, T., Hedrich, R. and Becker, D. (2010) Early signaling through the Arabidopsis pattern recognition receptors FLS2 and EFR involves Ca^{2+}-associated opening of plasma membrane anion channels. Plant J. **62**, 367-378
46 Nagai, T., Yamada, S., Tominaga, T., Ichikawa, M. and Miyawaki, A. (2004) Expanded dynamic range of fluorescent indicators for Ca^{2+} by circularly permuted yellow fluorescent proteins. Proc. Natl. Acad. Sci. U.S.A. **101**, 10554-10559
47 Monshausen, G. B., Messerli, M. A. and Gilroy, S. (2008) Imaging of the yellow cameleon 3.6 indicator reveals that elevations in cytosolic Ca^{2+} follow oscillating increases in growth in root hairs of Arabidopsis. Plant Physiol. **147**, 1690-1698
48 Rincón-Zachary, M., Teaster, N. D., Sparks, J. A., Valster, A. H., Motes, C. M. and Blancaflor, E. B. (2010) Fluorescence resonance energy transfer-sensitized emission of yellow cameleon 3.60 reveals root zone-specific calcium signatures in Arabidopsis in response to aluminum and other trivalent cations. Plant Physiol. **152**, 1442-1458
49 Qi, Z., Stephens, N. R. and Spalding, E. P. (2006) Calcium entry mediated by GLR3.3, an Arabidopsis glutamate receptor with a broad agonist profile. Plant Physiol. **142**, 963-971
50 Wurzinger, B., Mair, A., Pfister, B. and Teige, M. (2011) Cross-talk of calcium-dependent protein kinase and MAP kinase signaling. Plant Signal. Behav. **6**, 8-12

Figure legends

Figure 1 flg22, elf18 and chitin induce Ca^{2+} influx from the apoplast.
10 to 12-day-old aequorin-expressing *Arabidopsis* seedlings were pretreated for one hour with 1 mM $LaCl_3$ (A-C) or 10 mM EGTA (D). The measurements were started and after two minutes, flg22 (1 µM, A and D), elf18 (1 µM, B) or chitin (0,1 mg/ml, C) were automatically added. The luminescence originating from the seedlings was followed in time and Ca^{2+} concentrations were calculated according to [25]. The grey marking delineates the spike in luminescence caused by the injection of the MAMPs. Shown are average $\Delta[Ca^{2+}]$ values (± standard deviation) after correction for basal Ca^{2+} levels before MAMP addition. Curves shown are based on representative measurements of 4 to 6 seedlings per treatment. Each experiment was at least performed three times with similar results.

Figure 2 No apparent contribution from internal Ca^{2+} stores and VGCCs to the flg22-, elf18- and chitin-induced $\Delta[Ca^{2+}]$.
10 to 12-day-old aequorin-expressing *Arabidopsis* seedlings were pretreated for one hour with 10 µM U73122 (*A* and *B*), 200 µM Ruthenium Red (*C* and *D*), 100 µM tetracaine (*E*) or 100 µM nifedipine (F). The measurements were started and after two minutes, flg22 (1 µM, *A*, *B*, *E* and *F*), elf18 (1 µM, *C*) or chitin (0,1 mg/ml, *D*) were automatically added. The luminescence originating from the seedlings was followed in time and Ca^{2+} concentrations were calculated according to [25]. The grey marking delineates the spike in luminescence caused by the injection of the MAMPs. Shown are average $\Delta[Ca^{2+}]$ values (± standard deviation) after correction for basal Ca^{2+} levels before MAMP addition (*B*-*F*) or absolute $[Ca^{2+}]$ (*A*). Curves shown are based on representative measurements of 4 to 6 seedlings per treatment. Each experiment was at least performed three times with similar results.

Figure 3 Modulation of cNTP signalling does not influence the flg22-, elf18- or chitin-induced $\Delta[Ca^{2+}]$.
10 to 12-day-old aequorin-expressing *Arabidopsis* seedlings were pretreated for one hour with 1 mM alloxan (A), 200 µM dideoxyadenosine (B). The measurements were started and after two minutes, flg22 (1 µM) was automatically added. The luminescence originating from the seedlings was followed in time and Ca^{2+} concentrations were calculated according to [25]. The grey marking delineates the spike in luminescence caused by the injection of the MAMPs. Shown are average $\Delta[Ca^{2+}]$ values (± standard deviation) after correction for basal Ca^{2+} levels before MAMP addition. Curves shown are based on representative measurements of 4 to 6 seedlings per treatment. Each experiment was at least performed three times with similar results.

Figure 4 Modulation of iGluR-like channel function reduces the flg22-, elf18- or chitin-induced $\Delta[Ca^{2+}]$.
10 to 12-day-old aequorin-expressing *Arabidopsis* seedlings were pretreated for one hour with 1 mM AP-5 (A and B), 1 mM kynurenic acid (C), 1 mM L-glutamate (D and E), different amino acids (F) or a range of L-glutamate concentrations (G). The measurements were started and after two minutes, flg22 (1 µM) was automatically added. The luminescence originating from the seedlings was followed in time and Ca^{2+} concentrations were calculated according to [25]. Shown are average $\Delta[Ca^{2+}]$ values (± standard deviation) after correction for basal Ca^{2+} levels before MAMP addition (B, C and E) or absolute $[Ca^{2+}]$ (A, D). The histogram (F) shows the steady state $[Ca^{2+}]$ or the $\Delta[Ca^{2+}]$ (nM) after flg22 (1 µM), elf18 (1 µM) or chitin (0.1 mg/ml) stimulus at the maximum of the Ca^{2+} transient after pretreatment for 1 hour with 1mM L-alanine [A], L-cysteine [C], L-aspartate [D], L-glutamate [E], glycine [G], L-histidine [H], L-lysine [K], L-leucine [L], L-glutamine [Q], L-tryptophan [W] and the mock control [-]. Values represent averages of 3 to 6 biological replicates with 6 individual seedlings per replicate. Statistical significant differences were assessed using a Student's t-test with treatments compared to the mock control ($P<0.05$) (G). For the L-glutamate concentration range (G), the average basal Ca^{2+} concentration was determined using the average Ca^{2+} concentration of the time points before injecting flg22. The ΔCa^{2+} value was calculated using background-corrected Ca^{2+} concentrations and the values between 3.5 and 5 minutes were averaged. Each experiment was at least performed three times with similar results. Curves shown are based on representative measurements of

4 to 6 seedlings per treatment (A-E) or the mean of n=3 independent experiments (F). Error bars in the graphs represent the SD (A-E) or the standard error of the mean (F-G).

Figure 5 Modulation of iGluR-like channel function or inhibition of Ca^{2+} influx from the apoplast affects MAPK activation.
10-12-day-old *Arabidopsis* Col-0 seedlings were pretreated for one hour with 1 mM L-glutamate (A-C), 1 mM kynurenic acid (A and B), 1 mM CNQX (A and B), 1 mM $LaCl_3$ (C) or 10 mM EGTA (C). Time point 0 minutes was harvested before MAMP addition. 1 mM L-glutamate (A) or 0,1 mg/ml chitin (B and C) were added and after 5 minutes and 15 minutes samples were taken and analysed for MAPK activation as previously described [26]. Per sample 10-12 seedlings were used. Arrows mark the activated MAPKs on the blots. Experiments were repeated two or three times with similar results.

Figure 6 iGluR signalling and cNTP signalling act additively in elf18-induced Ca^{2+} influx.
10-12-day-old aequorin expressing *Arabidopsis* seedlings (*A*) and Col-0 wild type seedlings (*B*) were pretreated for one hour with 1 mM L-glutamate, 1 mM alloxan or a combination of both. Aequorin based Ca^{2+} measurements (A): Two minutes after initiation of luminescence detection, elf18 (1 µM) was automatically added. The luminescence originating from the seedlings was followed in time and Ca^{2+} concentrations were calculated according to [25]. The grey marking delineates the spike in luminescence caused by the injection of the MAMPs. Shown are the averages of the mean $\Delta[Ca^{2+}]$ of >3 biological replicates per treatment after correction for base Ca^{2+} levels with the standard error of mean. MAPK assays (B): Time point 0 minutes was harvested before MAMP addition; then, 1 µM elf18 was added and after 5 minutes and 15 minutes samples were taken and analysed for MAPK activation as previously described [26]. Per sample 10-12 seedlings were used. Arrows mark the activated MAPKs on the blots. Experiments were repeated two or three times with similar results.

Figure 7 Modulation of iGluR-mediated Ca^{2+} influx inhibits MAPK- and CDPK-dependent defense gene transcript accumulation.
10-12-day-old *Arabidopsis* Col-0 wild type seedlings were pretreated for one hour with 1 mM L-glutamate or 1 mM kynurenic acid. Time point 0 minutes was harvested before MAMP addition and flg22 (1 µM), elf18 (1 µM) or chitin (0,1 mg/ml) were added. Samples were taken at 30 and 60 minutes after MAMP addition and prepared for quantitative RT-PCR. PCRs were performed with primers specific for FRK1 and PHI-1 [29] and the reference gene At4G26410, The data were normalized to the reference gene and the value at time point 0 minutes of the non-pretreated samples was set to 1. The mean relative transcript accumulation of FRK1 (A) and PHI-1 (B) are presented in the graphs. Error bars represent the standard deviation of three technical replicates. The experiment was repeated three times yielding similar results.

Figure 8 A model for MAMP-triggered iGluR-mediated Ca^{2+} influx in *Arabidopsis thaliana*.
The scheme depicts a potential scenario based on our experimental results. CaM-Ca^{2+}, activated (Ca^{2+}-bound) calmodulin. For further explanation see main text.

Table 1 Overview of alterations in intracellular Ca^{2+}levels upon MAMP treatment in the presence of compounds modulating Ca^{2+} transport [a].

	flg22			elf18			Chitin			
Pre-treatment	**Base**	**Peak**	**Rec**	**Base**	**Peak**	**Rec**	**Base**	**Peak**	**Rec**	**Action**
-	=	=	=	=	=	=	=	=	=	
$LaCl_3$	=	0	=	=	0	=	=	0	=	Blocks Ca^{2+} influx channels
EGTA	↑	0	=	↑	0	=	↑	0	=	Chelates extracellular Ca^{2+}
U73122	↑	=	=	↑	=	=	↑	=	=	Inhibits phospholipase C
Neomycin	↑	↓	=	↑	↓	=	↑	=	=	Inhibits phospholipase C
Ruthenium Red	↑	↓	=	↑	↓	=	↑	↓↓	=	Inhibits ryanodine receptor-controlled CICR and influx via plasma membrane-resident channels
Tetracaine	=	↑	= ^^	=	↑	= ^^	=	↑	= ^^	Inhibits ryanodine receptor-controlled CICR release
Diltiazem	=	=	= ^^	=	=	= ^^	=	=	= ^^	L-Type VGCC inhibitor
Verapamil	=	=	= ^^	=	=	= ^^	=	=	= ^^	L-Type VGCC inhibitor
Nifedipine	=	=	→	=	↓	→	=	↓	→	L-Type VGCC inhibitor plus inhibitor of ABC transporters
Alloxan	=	=	=	=	↓	=	=	↓	=	Adenylate cyclase inhibitor
Dideoxyadenosine	=	=	=	=	↓	=	=	↓	=	Adenylate cyclase inhibitor
L-glutamate	↑	↓↓	=	↑	↓↓	=	↑	↓↓	=	iGluR agonist
AP-5	↑	↓↓	=	↑	↓↓	=	↑	↓↓	=	iGluR NMDA antagonist (L-glutamate binding site)
AP-7	↑	↓↓	=	NT	NT	NT	NT	NT	NT	iGluR NMDA antagonist (L-glutamate binding site)
Kynurenic acid (KA)	↑	↓↓	=	↑	↓↓	=	↑	↓↓	=	iGluR non-selective NMDA/non-NMDA antagonist (glycine binding site)
MK-801	=	=	=	=	=	=	=	=	=	iGluR NMDA receptor antagonist (binds in pore)
DNQX	=	=	=	=	=	=	=	=	=	iGluR non-NMDA receptor antagonist (binds in pore)
CNQX	=	=	=	=	=	=	=	↓	=	iGluR non-NMDA receptor antagonist (binds in pore)
Alloxan + L-glutamate	↑	↓↓	=	↑	↓↓	=	↑	↓↓	=	
Alloxan + KA	↑	↓↓	=	↑	↓↓	=	↑	↓↓	=	
DDA +L- glutamate	↑	↓↓	=	↑	↓↓	=	↑	↓↓	=	
DDA + KA	↑	↓↓	=	↑	↓↓	=	↑	↓↓	=	

[a] Qualitative evaluation of response of at least 3 replicates. = same as non-treated, 0 no Ca^{2+} transient visible, ↑ $[Ca^{2+}]$ increased compared to non-treated, → delayed recovery $[Ca^{2+}]$ after application MAMP compared to non-treated, ↓ small reduction $\Delta[Ca^{2+}]$ in peak compared to non-treated, ↓↓ strong reduction $\Delta[Ca^{2+}]$ in peak compared to non-treated , ^^ occurrence of random increases in $[Ca^{2+}]$ during recovery phase after MAMP application, NT, not tested

Figure 1

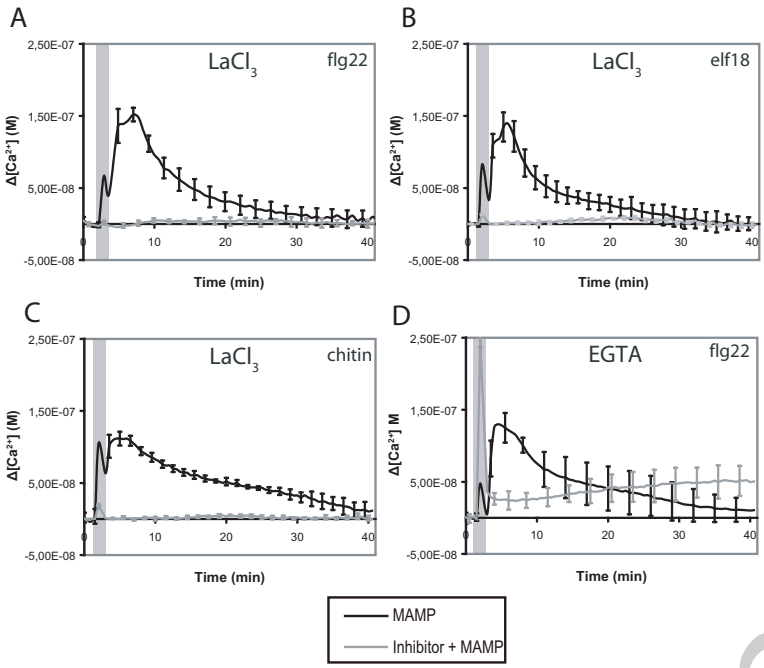

Biochemical Journal Immediate Publication. Published on 18 Aug 2011 as manuscript BJ20111112

Figure 2

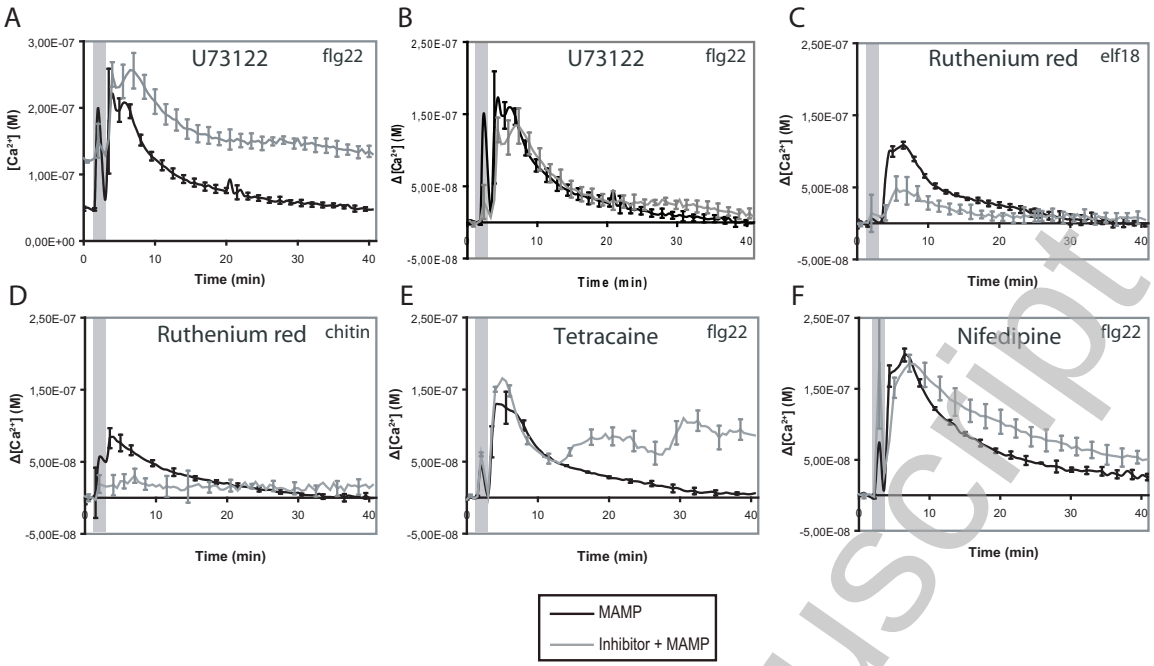

Figure 3

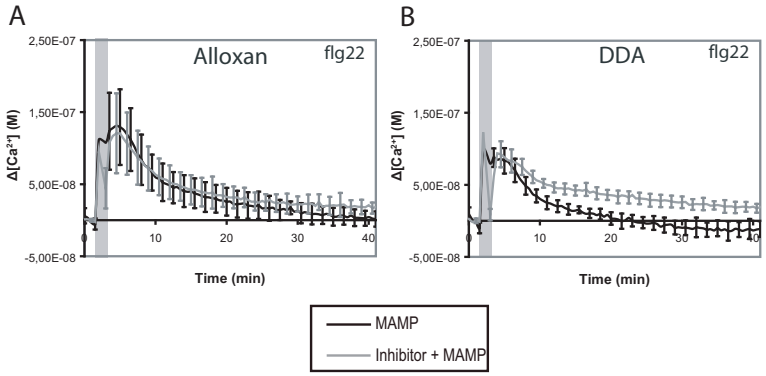

Biochemical Journal Immediate Publication. Published on 18 Aug 2011 as manuscript BJ20111112

Figure 4

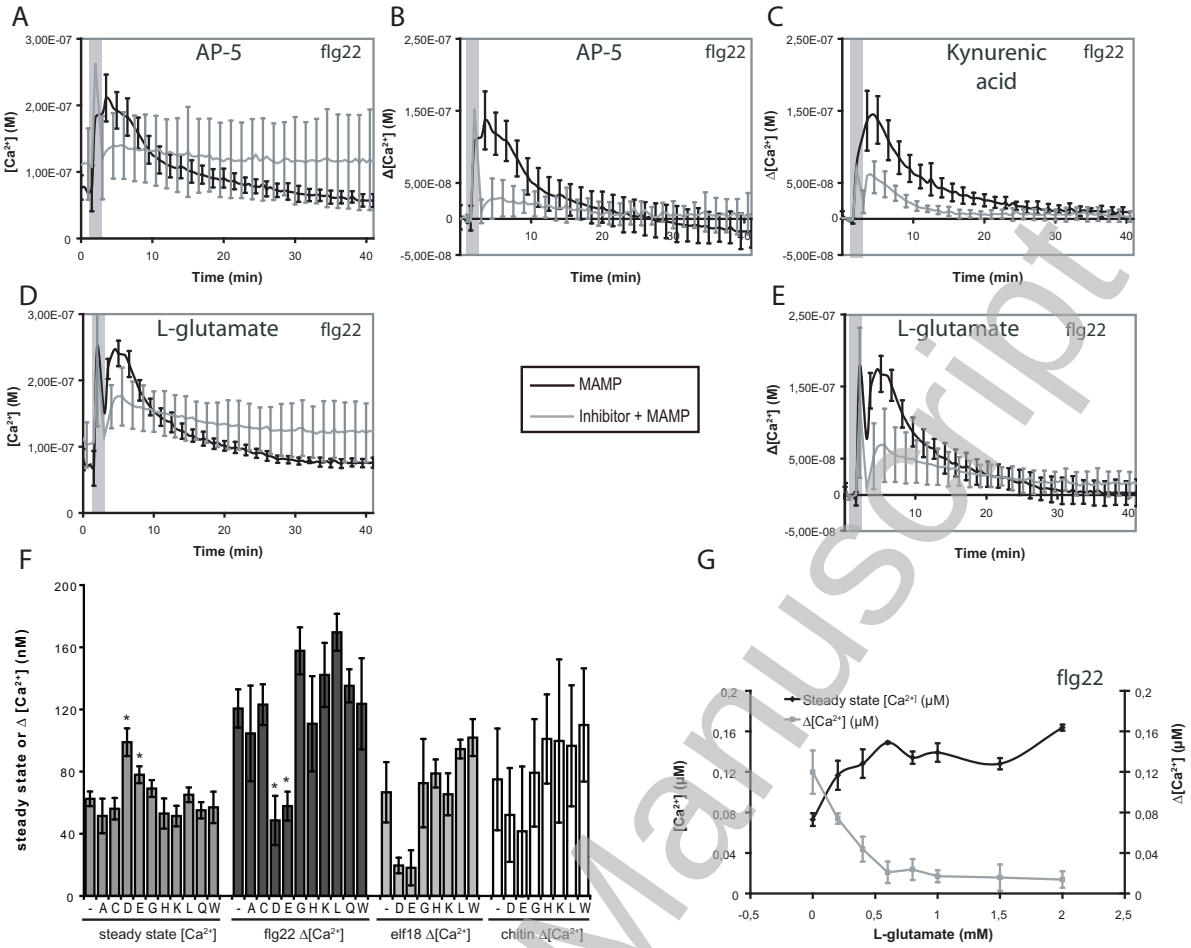

Figure 5

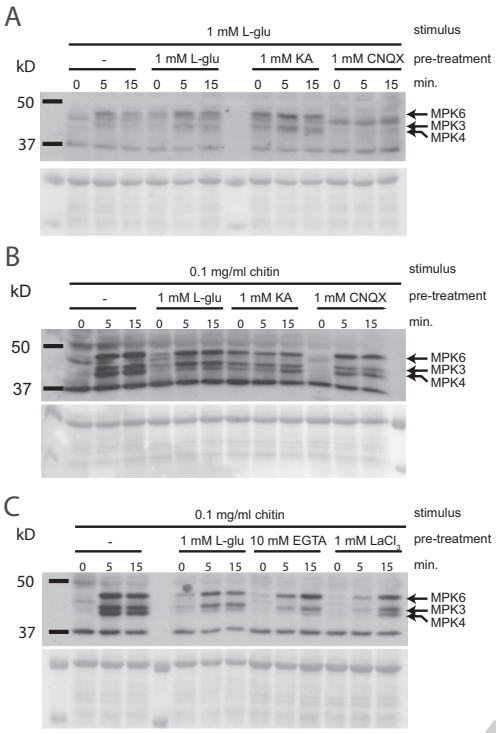

Figure 6

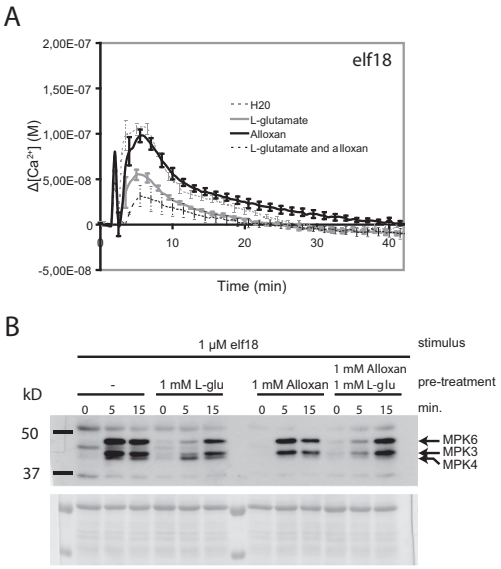

Figure 7

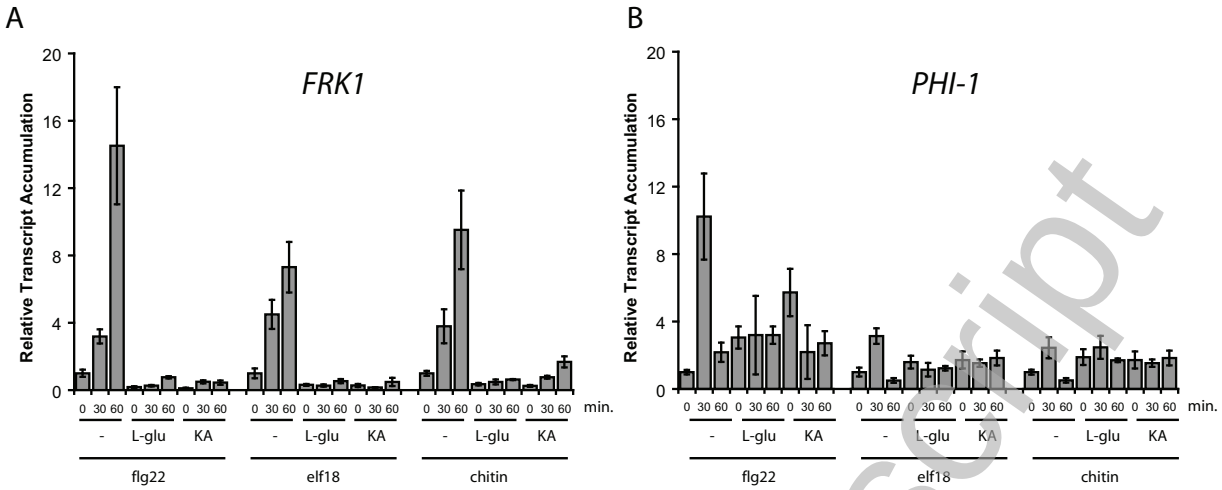

Figure 8